

Evaluating the Efficacy of Shear Connectors in H Steel Sections Embedded in Concrete

Alaulddin A. AL-Jafal *

alaulddin.21enp60@student.uomosul.edu.iq

Suhaib Y. AL-Darzi *

suhaib.qasim@uomosul.edu.iq

* Civil Engineering Department, College of Engineering, University of Mosul, Mosul, Iraq

Received: May 2nd, 2024 Received in revised form: July 29th, 2024 Accepted: September 9th, 2024

Abstract

this study is focusing on H steel sections embedded in concrete by evaluating various shear connectors, including headed studs, bolts, steel angles, perfobonds, and self-connected variants. This comprehensive examination of nine specimens aims to understand their load-bearing capacity, failure mechanisms, and overall performance in structural composite connections. The paper thoroughly compares and analyzes the load-slip curves, average initial shear stiffness, ultimate load, ductility, and fracture energy for these connectors. The research highlights self-connected connectors with rebars passing through flanges demonstrating substantial increases in ultimate load (41 %) in comparison to natural bond only, and maintaining ductility post-peak. Moreover, through this study it has been found that when shear studs and shear angles are designed for equivalent loads exhibit remarkably similar performance. Additionally, adding extra connectors to the web of H-sections enhances load capacity and stiffness but reduces ductility. The double shear in 10 mm diameter 8.8 bolted (with two nuts inside and outside flange) connectors raise the ultimate load but shift the curve of load slip from ductile to brittle in comparison with the same diameter studs.

Keywords:

Shear connectors; load-slip; Perfobond; studs; self-connected.

This is an open access article under the CC BY 4.0 license (<http://creativecommons.org/licenses/by/4.0/>).

<https://rengj.mosuljournals.com>

Email: alrafidain_engjournal3@uomosul.edu.iq

1. INTRODUCTION

The efficiency of shear connectors is crucial for maintaining the structural integrity of steel-reinforced concrete (SRC) constructions, pivotal components are facilitating composite action between steel sections and concrete. These connectors play a fundamental role in harnessing steel's tensile strength alongside concrete's compressive strength, thereby fortifying the overall structural resilience [1]. The requirements for bond stress and mechanical connections are critical components in concrete-encased steel constructions. The behavior of SRC elements is profoundly swayed by bond stress, mandating the provision of shear connectors when the demanded bond stress exceeds the capacity [2]. However, there is still a lack of comprehensive research to evaluate them against one another.

In the realm of engineering, the selection of connectors transcends mere strength considerations, extending to factors such as ductility, sustainability, ease of assembly, and cost-

effectiveness [3]. According to Eurocode standards, shear connectors should exhibit slip at 90% of the ultimate load exceeding 6 mm to qualify as ductile—a criterion critical for ensuring ample ductility and energy absorption capacity in structural connections [4]. This study encompasses a spectrum of connector types, including headed studs, bolts, steel angles, perfobonds, and innovative self-connected variants. Through rigorous push-out tests on H steel sections embedded in concrete, The evaluation of these connectors provides insights into their load-bearing capacity and failure mechanisms. [5]. The load-slip relationship governs the linear and nonlinear characteristics of shear connections in the design of SRC structures. [6].

Shear connectors in composite construction, such as headed stud shear connectors, are chosen for their significant shear capacity and load-slip behavior. [7]. Despite being subject to factors, like hole slip and thread penetration [8], bolted shear connectors approach the performance of traditional welded studs, achieving nearly 95% of the latter's shear resistance under static loads. Their substantial fatigue strength makes them suitable for uses that require durability, such as reinforcing bridges [9]. Although bolted stud connectors have a somewhat lower shear resistance than headed stud connectors, their performance characteristics are harmoniously blended, highlighting their value in specialized structural applications. [10].

In many construction situations, self-connected connectors are widely used, particularly in buildings and bridges where smooth component integration is crucial. Highly regarded for their effectiveness in transferring load, these connections are commonly used in cable-stayed bridges. [11]. The pioneering Perforated Web Connection (PWC) in Concrete-Encased Steel (CES) bridges augments the shear-slip response, piloting a transition from brittle to ductile failure mode [12]. For perfobond shear connectors, a recommended strip thickness exceeding 9 mm ensures a double shear failure in the rebar—a specification pivotal for structural robustness [13]. Finite element analysis affords intricate insights into connector behavior under diverse loading conditions, supporting the comprehension of their mechanical properties and facilitating prognostications of long-term performance [14].

In vertical concrete casting for structures, like columns or pile caps, the susceptibility to concrete settlement or air pockets beneath shear connectors is heightened, particularly for angle-type connectors due to their larger surface area, this juxtaposes slabs where horizontal concrete casting mitigates such concerns. Vigilant assessment and mitigation of these risks are indispensable for preserving structural integrity [15].

Data was normalized by dividing the maximum force that each shear connector could sustain by the strength of the material when various materials with differing capacities were used for the connectors. However, this method isn't fully equitable since the shear strength capability is the most important aspect, as it's taken into account for this research [16].

1.1 Research significance

This study integrates practical experiments with a comprehensive analysis to thoroughly evaluate various types of shear connectors with similar shear capacity. The primary objective is to closely examine these connectors and discern their distinctive attributes compared to one another. It meticulously examines and contrasts load-slip curves, average initial shear stiffness, ultimate load, ductility, and fracture energy.

2. EXPERIMENTAL PROGRAM

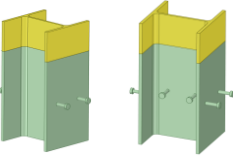
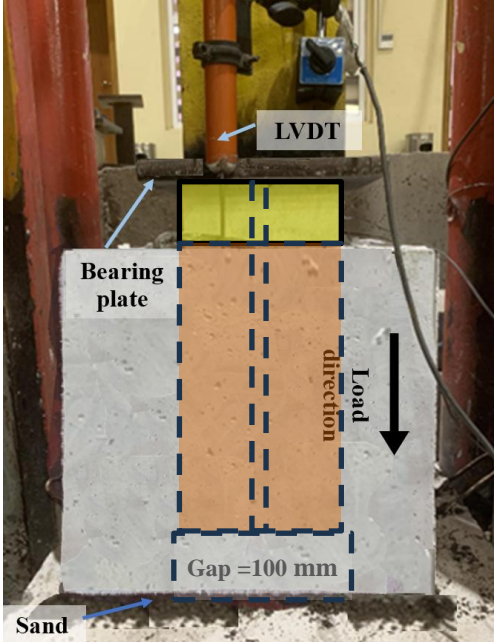
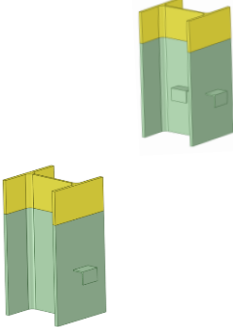
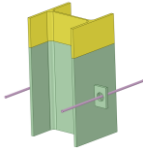
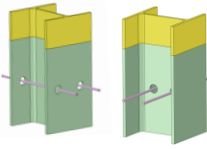
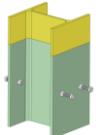
2.1 Materials

The materials and components used in the specimens were carefully selected to ensure their reliability and integrity. The Badush expansion facility provided the ordinary Portland cement Type 1 [17], and Mosul City/Knhash provided fine aggregate and naturally rounded river gravel that complied with IQS:45/2010 regulations [18]. Steel reinforcement was composed of stirrup bars ($\text{Ø}10$ mm), transverse reinforcement ($\text{Ø}8$ mm), and longitudinal reinforcement ($\text{Ø}12$ mm) deformed bars. A particular H steel section measuring H 200*200*7*10 mm dimensions confirmed following ASTM A36 standards was selected for its load-carrying capabilities [19]. Material properties of the five different types, as they represent some of the most widely used connections, are shown in Table 1. and are graphically configured as depicted in Table 2., this all-encompassing strategy guarantees careful inquiry.

Table 1. Connectors material properties

No.	connection	Specimen name	Dimension mm	Yield Stress	Ultimate Strength
1	Shear stud	HS1, HS2	10*50 shank 7*19 Head	429	661
2	Steel Angle	HA1, HA2	36*36*3 mm Length 60 mm	369	463
3	Perfobond Plate	HP1	70*50*10 mm Hole $\text{Ø}30$ mm	288	457
4	Self-Connected	HSF, HSW	Bar $\text{Ø}8$ mm	445	625
5	Bolt	HB1, HB2	75 $\text{Ø}10$ mm	850	905

Table 2. Connectors configuration

Specimens	Connectors configuration	Test Configuration for control H00
HS1, HS2 (studs)		
HA1, HA2 (angle)		
HP1 (perfobond)		
HSF, HSW (self-connected)		
HB1 (bolt and nuts)		

2.2 Design of specimens

The nine specimens involved embedding an H steel section within different connections as shown in Table 2. embedded in 400x400 mm concrete block. The concrete which has been used had a compressive strength of 28 MPa, with the steel section embedded to a depth of 300 mm and leaving a 100 mm gap beneath it. The purpose of this setup was to assess the effectiveness of different mechanical connections, such as headed shear studs, angle shear connections, perfobond, self-connected methods, and bolt with nuts configurations, the detail of each specimen connection is shown in Table 3. These connections were designed to achieve an ultimate shear value of approximately 65 kN \pm 3 kN, ensuring consistency for comparative analysis of steel-concrete interaction under various stress

conditions. The following equation was used to design the connectors.

- 1- Headed shear studs: $V_u = 0.5A_s\sqrt{E_c f'_c} \leq A_s f_u$
----- AASHTO Eq. (1) [20]
 - 2- Angle shear connectors:
 $V_u = 0.3(t_f + 0.5t_w)L_a\sqrt{E_c f'_c}$ ----- AISC (16.1-106) Eq. (2)[21]
 - 3- Perfobond connectors:
 $V_u = 1.76 \times \frac{\pi}{4}(D^2 - d_r^2)f'_c + 1.38 \frac{\pi}{4}d_r^2 f_{ry}$ --
----- Zhao and Liu Eq. (3) [22]
 - 4- Self-connected is used as equation 3 when the web is perforated
 - 5- Bolted connectors with the same diameter and height as studs (10mm x 50mm).
- The first equivalent group A (HS1, HA1, HP1, HSW)

The second equivalent group B (HS2, HA2, HSF, HB1)

Table 3 Specimens details

specimen	Shear connectors	Location	Connection Details
HS1	4 studs	2 Attach to each Flange	Shaft $\Phi 10 * 43\text{mm}$, Head $\phi 19 * 7\text{ mm}$
HS2	8 studs	2 Attach to each Flange 2 Attach to each side of the Web	
HA1	2 angles	one attached to each Flanges	L 36*36*3 mm Long 60 mm
HA2	4 angles	one attached to each Flanges one attached to each side of the Web	
HP1	perfobond	Strip attached to each Flanges	Strip 70*70*7 mm, Hole 30 mm, rebar $\phi 8\text{mm}$
HSW	Self-Connected	Rebar pass throw web	Two Hole in web $\phi 30\text{ mm}$, rebar $\phi 8\text{ mm}$
HSF	Self-Connected	Rebar pass throw Flanges	Two Hole each flange $\phi 30\text{ mm}$, rebar $\phi 8\text{ mm}$

2.3 Test setup and instrumentation

The test setup was carefully designed to measure the performance of each specimen under controlled conditions. A Universal Test Machine, equipped with a hydraulic jack system of 1000 kN capacity, formed the core of the experimental setup. Each specimen was placed on this machine, ensuring uniform load distribution through a steel bearing plate. To minimize friction, a fine sand layer was spread beneath each specimen. Alignment was meticulously verified using a plumb bob between the two vertical surfaces, and a bubble level was employed for continuous monitoring. Linear Variable Differential Transformers (LVDTs) were attached to each specimen to measure differential displacement. An automated data logger, TDS-530, was used to collect and record data from strain gauges, LVDTs, and the load cell. This setup allowed for precise control and monitoring of the load applied, ensuring a thorough evaluation of the specimen's structural behavior under various loading conditions.

3. EXPERIMENTAL RESULT AND DISCUSSION

3.1 Load-Slip relationship comparisons for group A

Figure 1 presents a comparison of the load slip properties of the HS1, HA1, HP1, and HSW specimens against the H00 specimen, which depends exclusively on natural bonding. Despite being theoretically engineered to withstand the same ultimate shear loads, the observed behaviors of these specimens differ, as detailed in the subsequent sections:

- 1- H00 (control specimen): An important insight into the load-slip behavior of steel-concrete interfaces is provided, the control specimen is distinguished by its absence of mechanical connections and reliance only on natural bonds, such as chemical adhesion and friction. With an Ultimate Load of 307 kN, this specimen set a fundamental standard by which additional specimens may be evaluated. It displayed a Slip of 0.67 mm at Ultimate Load, indicating that the displacement is at maximum load. The connection's intrinsic stiffness under initial loading conditions was shown by the measurement of the initial stiffness, which was 527 kN/mm. Furthermore, the reported Fracture Energy of 5508 indicates that the specimen

possesses the ability to absorb energy up to the point of residual load stabilized.

- 2- HS1(two studs attached to each flange): demonstrated superior performance compared to the natural bond H00. It reached an Ultimate Load of 337 kN, which is 10% higher than H00, and a significantly increased Slip at Ultimate Load of 6.1 mm, marking an 810% rise and indicating an enhancement in ductility. Its Initial Stiffness improved by 28% to 673 kN/mm, and Fracture Energy rose by 12% to 6168. Notably, it showed an increase in post-peak ductility, with a 7.56 mm slip at 90% of the ultimate load. These results suggest that the studs significantly boost both load capacity and flexibility, beneficial for applications requiring high energy absorption and deformation tolerance.
- 3- HA1(Single steel angle attached to each Flanges): the specimen outperformed the H00 natural bond specimen in a significant way. With an Ultimate Load of 328 kN, 7% more than H00, it demonstrated a marginally but significantly higher load capacity. With a significant 558% increase, the Slip at Ultimate Load was measured at 4.41 mm, indicating an improvement in ductility. The initial stiffness of the material increased by 19% to 627 kN/mm, referring to a considerable improvement. With a 10 % rise to 6062, Furthermore, at 90% of the ultimate load, HA1 demonstrated post-peak ductility with a slip of 6.20 mm.
- 4-HP1(Perfobond): The specimen incorporating a Perfobond strip attached to each flange, demonstrates distinct characteristics compared to other specimens. It achieved an Ultimate Load of 337 kN, matching HM0S1 and marking a 10% increase over HM000. However, it exhibited a significantly lower Slip at the Ultimate Load of just 0.22 mm, a 67% decrease from H00, indicating a reduction in ductility. The Initial Stiffness of HP1 was 1360 kN/mm, showing a substantial 158 % increase. Its Fracture Energy also saw a considerable rise to 7300, denoting a 33% enhancement in energy absorption. Notably, HP1 did not exhibit ductility post-peak, with a slip of only 4.20 mm at 90% of the ultimate load. The perfobond connector in HP1 results in high stiffness and load capacity but limits ductility, suggesting that its application might be constrained in scenarios where high deformation capacity is essential.
- 5-HSW (Self-connected): With two ϕ 8 mm rebars going through two ϕ 30 mm holes in the web, the specimen displays special performance characteristics. Its ultimate load of 383 kN, which represents a noteworthy 25% increase over H00, suggesting that its load-bearing capacity has improved significantly. Its Slip at

Ultimate Load, however, was just 0.27 mm—60% less than H00—indicating a decline in ductility. With an initial stiffness of 1500 kN/mm, HSW had the highest initial stiffness of all the previous specimens tested, marking a significant increase of 185%. Its fracture energy increased respectably as well, rising to 6150 (11%), pointing a better absorption for energy. Even with these strengths, HSW showed only a small slide of 0.49 mm at 90%

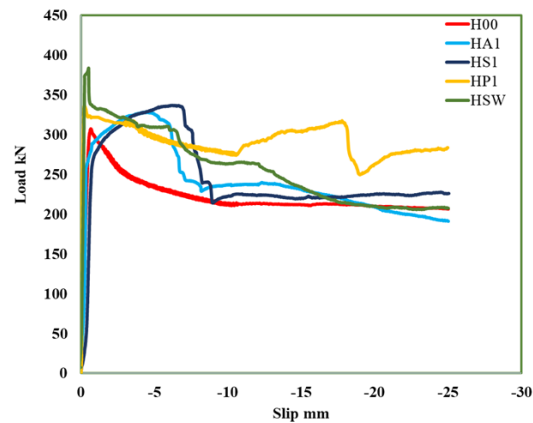


Figure 1. Load-Slip for group A

Despite minor variations, with HS1 slightly outperforming HA1 in certain aspects, their overall performance is remarkably similar. HP1 and HSW, while providing higher load capacities and stiffness, exhibited reduced ductility. HS1 and HA1 are suitable for scenarios requiring both strength and flexibility, whereas HP1 and HSW are better suited for situations where high load capacity and stiffness are prioritized over ductility.

3.2 Load slip relationship for group B:

Figure 2 illustrates a comparative analysis of the load slip characteristics for the HS2, HA2, HB1, and HSF samples with the H00 specimen. It's important to highlight that the inclusion of the HB1 in this comparison is significant, as the presence of nuts both inside and outside the flange in this specimen contributes to an enhanced resistance, thereby elevating the ultimate load capacity.

1-HS2 (8 Studs): HS2 demonstrated a marked improvement in the steel-concrete interface, with a 54 % increase in Ultimate Load to 474 kN and a 403% rise in Slip at Ultimate Load to 3.37 mm. The Initial Stiffness increased by 142% to 1275 kN/mm, signaling a stiffer connection. Fracture Energy also increased by 52% to 8360, but the specimen lacked post-peak ductility, with only 4.86 mm slip at 90% of the ultimate load.

2-HA2 (4 Angles): HA2, with four angle connectors, saw a 28% increase in Ultimate Load to 392 kN and a 198% rise in Slip at

Ultimate Load to 2.0 mm. Initial Stiffness improved by 35% to 711 kN/mm, and Fracture Energy increased by 13% to 6220. However, HA2 showed limited post-peak ductility, with a 4.33 mm slip at 90% of the ultimate load.

3-HSF (Self-connected): The HSF specimen, with self-connected rebar through flanges, achieved a 41% increase in Ultimate Load to 433 kN, a 428% increase in Slip at Ultimate Load to 3.54 mm, and a 160% rise in Initial Stiffness to 1371 kN/mm. It also showed the highest increase in Fracture Energy by 59% to 8763, and maintained ductility post-peak with a 6.10 mm slip at 90% of the ultimate load.

4-HBI (Bolts): HBI, featuring bolted connections, reached an Ultimate Load of 394 kN, a 28% increase, but had a reduced Slip at an Ultimate Load of 0.37 mm, showing lesser ductility. The Initial Stiffness rose by 119% to 1152 kN/mm, and Fracture Energy increased by 56% to 8581. However, it showed a limited post-peak ductility with a 0.59 mm slip at 90% of the ultimate load.

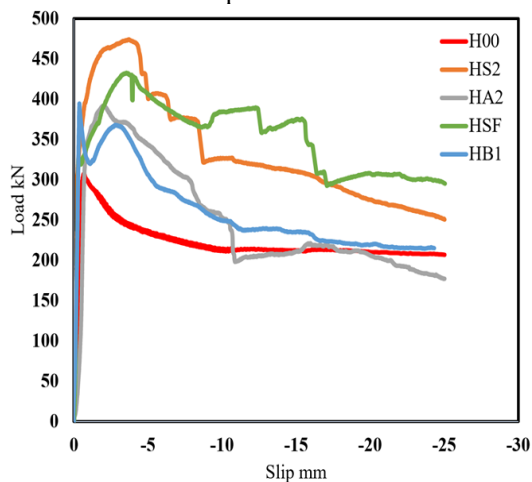


Figure 2. Load-Slip for group B.

Among Group B specimens, HS2 and HSF demonstrated significant improvements in load capacity and energy absorption, with HS2 leading in ultimate load and HSF in energy absorption and ductility. HA2 offered moderate enhancements but lacked post-peak ductility. HBI showed an improvement in load capacity and energy absorption but had limited ductility, both at ultimate load and post-peak. Overall, each specimen presents a unique balance between load capacity, stiffness, energy absorption, and ductility, making them suitable for different structural applications.

3.3 Mode of failure

the mode of failure for the connection of specimens HS1 and HA1, Figures 3a. and 3b. respectively illustrates that both models

experienced shear connector failures at the welded ends, exhibiting a combination of flexural and shear failures. Despite vertical casting, there were no vacuums or air bubbles under the flanges due to fresh concrete consolidation. The mode failure reveals that these specimens, compared to the control H00, showed significant cracking. Two parallel longitudinal cracks developed along the flange faces at about 85% load, originating from the free end and progressing toward the center.



a. Shear stud failure



b. Angle failure

Figure 3. HS1&2 and HA1&2

For HS1, horizontal cracks connected the longitudinal ones between the studs at a load just above 307 kN, post reaching the ultimate load of 334 kN. As the load was reduced to 220 kN, diagonal cracks appeared. A similar pattern was noted in HA1. The increment in load application caused these cracks to extend towards the loaded end, and upon reaching the ultimate load of 328 kN, a horizontal fracture emerged at the angle connection, spreading to the specimen's sides. This was due to the bearing action of the angle connection. Around 324 kN, the cracks widened towards the edges, accompanied by audible signs of the connection breaking and vertical cracks in the web-side concrete.

The failure mode of the perfobond HP1 connection involving a 30 mm hole and an 8 mm deformed rebar was marked by distinct stages. Initial cracks appeared in the concrete at 60–70% of the ultimate load vertically extending from the bottom to the loaded end through the steel strip and bar location as shown in Figure 4. After reaching a peak load, the concrete's shear capacity decreased,

and the steel rebar started yielding, stretching up to 10 mm and then showing hardening resistance until a 20 mm displacement was reached,

indicating a single shear failure accompanied by an audible sound.

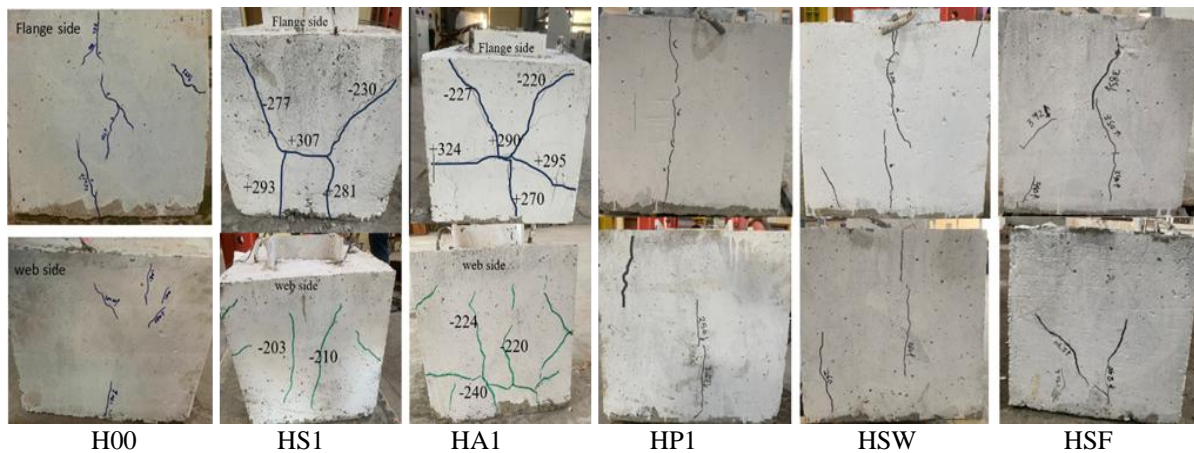


Figure 4. Specimen failure

The failure mode in self-connected HSW, where the rebar experienced double shear is shown in Figure 5. significantly increased the ultimate shear load in comparison to the perfobond connection. Despite the similarity in hole thickness (7 mm) between both the web and strip

properties and performance of different specimens under stress. In Table 4, the ultimate load capacity, slip at ultimate load, initial stiffness, and fracture energy are key parameters in assessing the structural integrity and materials response under load. The post-peak ductility, as observed in specimens HS1, HA1, and HSF, is a crucial attribute, indicating the ability of these materials to undergo significant deformation before failure - a desirable property in structures requiring flexibility and resilience.

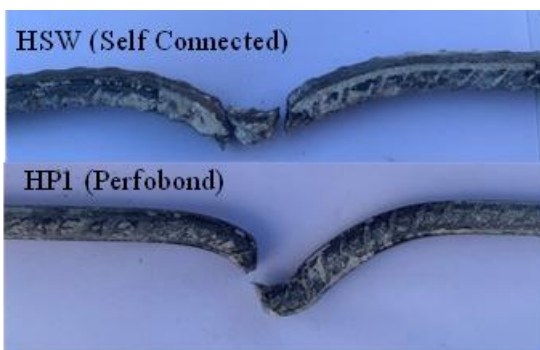


Figure 5. Rebar shear failure

in perfobond, the placement of the hole in the self-connected HSW differed significantly. It was located in a highly confined concrete zone within the flanges, which contrasted with the perfobond strip's position in a partially confined zone. This confinement increases in the HSW specimens restricted the rebar's ability to extend freely, unlike in the perfobond. As a result, the failure in the HSW system was more brittle, characterized by a sudden drop in load upon reaching its limit, unlike the more gradual failure progression observed in the perfobond connection.

3.4 Test result summary

Data from Tables 4 and 5 provide insightful observations about the mechanical

Table 5, with its focus on the percentage change in these properties compared to the control specimen H00, offers a perspective on how alterations in the specimen compositions affect their mechanical behavior. For example, the 54.40% increase in the ultimate load capacity and 142% increase in the initial stiffness for HS2 are indicative of an enhancement in structural strength and rigidity, which are vital in high-load-bearing applications. However, the slip increased at ultimate load for HS2 and HS1 (403% and 810%, respectively) points towards a potential trade-off between strength and stability, as a higher slip could imply less predictability in material behavior under peak stress conditions.

While modifications can enhance some mechanical properties like load capacity and stiffness, they can also lead to significant changes in other characteristics such as slip behavior and ductility. This highlights the importance of a balanced approach in material design, where the enhancement of one property should not overly compromise others, especially in applications where reliability and predictability under various load conditions are crucial.

Table 4. Summarize of results for all specimen

Specimens	Ultimate load (kN)	Slip at ultimate load (mm)	Initial stiffness (kN/mm)	Fracture energy	Slip at 90% Ultimate Load Post-Peak (mm)	Is Ductile Post-Peak
H00	307	0.67	527	5508	1.75	No
HS1	337	6.10	673	6168	7.56	Yes
HS2	474	3.37	1275	8360	4.86	No
HA1	328	4.41	627	6062	6.20	Yes
HA2	392	2.00	711	6220	4.33	No
HP1	337	0.22	1360	7300	4.20	No
HB1	394	0.37	1152	8581	0.59	No
HSW	383	0.27	1500	6150	0.49	No
HSF	433	3.54	1371	8763	6.10	Yes

Table 5. Percentage increment in comparison to the control specimen

Specimens	% Change in Ultimate Load	% Change in Slip at Ultimate load	% Change in Initial Stiffness	% Change in Fracture Energy
H00	0.00%	0.00%	0.00%	0.00%
HS1	10%	810%	28%	12%
HS2	54%	403%	142%	52%
HA1	7%	558%	19%	10%
HA2	28%	198%	35%	13%
HP1	10%	-67%	158%	33%
HB1	28%	-45%	118%	56%
HSW	25%	-60%	185%	11%
HSF	41%	428%	160%	59%

4. CONCLUSION

The research shows that different types of shear connectors (headed studs, bolts, steel angles, perfbonds, and self-connected variants) exhibit varying performance characteristics regarding load-bearing capacity and failure mechanisms.

1- Specimens incorporating connectors like headed studs and steel angles exhibited a substantial increase in both load capacity and ductility when compared to those relying solely on the natural bond. This outcome

highlights their potential for applications where demanding high energy dissipation and resistance to deformation are critical.

2- When shear studs and shear angles are designed to carry equivalent loads, they exhibit remarkably similar performance in terms of ultimate load capacity, shear stiffness, and energy absorption. Additionally, both types of connectors display comparable failure modes, albeit with minor variations.

3- The study also reveals that providing additional connectors to the web of H-sections, as seen in HS2 (with eight studs) and HA2 (with four angles), significantly enhances the load capacity and stiffness compared to HS1 and HA1, which have flange connectors only. However, this increase in strength and rigidity comes at the cost of ductility reduction.

4- The HS2 and HSF specimens showed higher increases in ultimate load and slip at ultimate load, compared to HA2. In particular, the self-connected connector (HSF) showed a 41% increase in ultimate load comparing to the natural bond and maintained ductility post-peak with a 6.10 mm slip at 90% of the ultimate load. It also showed a better post-peak ductility when compared to HS2 and HA2.

5- The double shear failure in HSW rebar with a 7 mm plate, instead of the required 9 mm, can be linked to its placement in a highly confined area within the flanges, unlike perfbond

connectors located in less confined zones outside the flange.

- 6- The double shear in 10 mm diameter 8.8 bolted (with two nuts inside and outside flange) connectors raise the ultimate load but shift the curve of load slip from ductile to brittle in comparison with the 10 mm stud HS1.
- 7- In future research, it would be beneficial to include a wider variety of specimens, materials, and other types of connections. Also, using a finite element program approach can help to overcome the limitations of physical specimens. This broader approach would improve the applicability of findings across different scenarios and support validation.

ACKNOWLEDGEMENTS

The authors wish to extend their profound gratitude to the Laboratory for Structural Materials Testing at Mosul University for their indispensable support and contributions throughout this study. Their assistance was crucial in facilitating the successful completion of the research.

REFERENCES

- [1] X. Wang, Y. Liu, Y. Li, Y. Lu, and X. Li, "Bond behavior and shear transfer of steel section-concrete interface with studs: Testing and modeling," *Constr. Build. Mater.*, vol. 264, Dec. 2020, doi: 10.1016/j.conbuildmat.2020.120251.
- [2] B. W. Charles Roeder, R. Chmielowski, A. Member, C. B. Brown, and H. Member, "SHEAR CONNECTOR REQUIREMENTS FOR EMBEDDED STEEL SECTIONS," *Eng. Struct.*, vol.125, pp.142-151,1999.
- [3] R. T. Pardeshi and Y. D. Patil, "Review of Various Shear Connectors in Composite Structures," *Adv. Steel Constr.*, vol. 17, no. 4, pp. 394–402, 2021, doi: 10.18057/IJASC.2021.17.4.8.
- [4] B. S. En, "Eurocode 2: Design of concrete structures Part 1-1: General rules and rules for buildings," *Eur. Comm. Stand.*, 2004.
- [5] J. Wei, Q. Yang, Y. Yu, Q. Wang, L. Zhou, and F. Chen, "Study of Bond-Slip Behavior and Constitutive Model of a New M-Section Steel-Skeleton Concrete," *Materials (Basel)*, vol. 15, no. 19, pp. 1–26, 2022, doi: 10.3390/ma15196776.
- [6] H. Meng, W. Wang, and R. Xu, "Analytical model for the Load-Slip behavior of headed stud shear connectors," *Eng. Struct.*, vol. 252, p. 113631, 2022.
- [7] P. Duratna, J. Bujnak, A. Bouchair, and F. Bahleda, "Behaviour and strength of headed shear stud connectors," *Commun. - Sci. Lett. Univ. Žilina*, vol. 15, no. 3, pp. 107–111, 2013, doi: 10.26552/com.c.2013.3.107-111.
- [8] D. S. Jung, S. H. Park, T. H. Kim, J. W. Han, and C. Y. Kim, "Demountable Bolted Shear Connector for Easy Deconstruction and Reconstruction of Concrete Slabs in Steel–Concrete Bridges," *Appl. Sci.*, vol. 12, no. 3, 2022, doi: 10.3390/app12031508.
- [9] F. Yang, Y. Liu, Z. Jiang, and H. Xin, "Shear performance of a novel demountable steel-concrete bolted connector under static push-out tests," *Eng. Struct.*, vol. 160, pp. 133–146, Apr. 2018, doi: 10.1016/j.engstruct.2018.01.005.
- [10] F. Yang, Y. Liu, H. Xin, and M. Veljkovic, "Fracture simulation of a demountable steel-concrete bolted connector in push-out tests," *Eng. Struct.*, vol. 239, no. April, p. 112305, 2021, doi: 10.1016/j.engstruct.2021.112305.
- [11] Q. Zhang, D. Jia, Y. Bao, Z. Cheng, Y. Bu, and Q. Li, "Analytical Study on Internal Force Transfer of Perfobond Rib Shear Connector Group Using a Nonlinear Spring Model," *J. Bridg. Eng.*, vol. 22, no. 10, pp. 1–11, 2017, doi: 10.1061/(asce)be.1943-5592.0001123.
- [12] X. Wang, Y. Liu, Y. Lu, and X. Li, "Shear transfer mechanism of perforated web connection for concrete encased steel structures," *Eng. Struct.*, vol. 252, p. 113418, 2022.
- [13] T. Hosaka, K. Mitsuki, H. Hiragi, Y. Ushijima, Y. Tachibana, and H. Watanabe, "An experimental study on shear characteristics of perfobond strip and its rational strength equations," *J. Struct. Eng. JSCE*, vol. 46, pp. 1593–1604, 2000.
- [14] J. Guo, Q. Shi, G. Ma, and T. Li, "Shear Behavior of Superposed Perfobond Connectors Considering Lateral Constraints," *Appl. Sci.*, vol. 12, no. 6, Mar. 2022, doi: 10.3390/app12063162.
- [15] S. R. Hicks, J. Cao, C. McKenzie, M. Chowdhury, and R. Kaufusi, "Evaluation of shear connectors in composite bridges," Wellington 6141, New Zealand, 2016.
- [16] V. Jayanthi and U. Gunasekaran, "Performance Evaluation of Different Types of Shear Connectors in Steel–Concrete Composite Construction," *Arch. Civ. Eng.*, vol. 64, pp. 97–110, 2018, doi: 10.2478/ace-2018-0019.
- [17] Iraqi Standard Specification I.Q.S, "Portland Cement," no. 5, 2010.
- [18] Iraqi Standard Specification I.Q.S, "The Aggregate of Natural Source Used in Concrete," no. 45, 2010.
- [19] L. Pallarés and J. Hajjar, "Headed steel stud anchors in composite structures, Part I: Shear," *J. Constr. Steel Res.*, vol. 66, no. 2, pp. 198–212, 2010, <http://www.sciencedirect.com/science/article/pii/S0143974X09002077>
- [20] American Association of State Highway and Transportation Officials, "AASHTO LRFD Bridge Design Specifications," 2017, p. 254.
- [21] American Institute of Steel Construction, AISC, "Specification for Structural Steel Buildings," pp. 1–612, 2010.
- [22] Z. Chen, "Experimental study of shear capacity of perfobond connector," vol. 29, no. 12, pp. 349–354, 2012.

تقييم فعالية موصلات القص في مقاطع فولاذية H المضمنة في الخرسانة

صهيب يحيى الدرزي *
suhaib.qasim@uomosul.edu.iq

علاء الدين عبد الرحمن الجفال*
alaulddin.21enp60@student.uomosul.edu.iq

قسم الهندسة المدنية، كلية الهندسة، جامعة الموصل، الموصل، العراق*

تاريخ الاستلام: 2 مايو 2024 استلم بصيغته المنقحة: 29 يوليو 2024 تاريخ القبول: 9 سبتمبر 2024

الملخص

الدراسة تركز على المقاطع الفولاذية H المضمنة في الخرسانة، تقييم موصلات القص المختلفة، بما في ذلك مسامير القص، والبراغي، وزوايا الصلب، والموصلات المثقبة، والأنواع المتصلة ذاتياً. تهدف هذه الدراسة التي تشمل تسعة عينات إلى فهم قدرة تحمل الحمل الخاصة بهذه الموصلات، والبيات الفشل، والأداء العام في توصيلات المركبات الهيكلية. والبحث يقوم بمقارنة وتحليل منحنيات الحمل مقابل الانزلاق، والصلابة القصوى الابتدائية، والحمل النهائي، واللدونة، وطاقة الكسر لهذه الموصلات. تسلط البحث الضوء على الموصلات المتصلة ذاتياً، حيث تمر قضبان التسليح عبر الفلانج للمقطع الفولاذي العرضية، والتي أظهرت زيادات كبيرة في الحمل النهائي (41%) مقارنة بالرابطة الطبيعي فقط، وحافظت على اللدونة بعد ذروة الحمل. كما يلاحظ البحث أنه عند تصميم مسامير القص وزوايا القص للمكافئ، فإنها تظهر أداءً متشابهاً بشكل ملحوظ. بالإضافة إلى ذلك، فإن إضافة موصلات إضافية إلى الويب H تعزز قدرة التحمل والصلابة لكنها تقلل من اللدونة. ويؤدي القص المزوج في براغي قطرها 10 ملم من النوع 8.8 (مع براغي داخلية وخارجية على الشريط العرضي) إلى زيادة الحمل النهائي ولكنه يحول منحنى الحمل مقابل الانزلاق من لدوني إلى هش بالمقارنة مع نفس قطر مسامير القص.

الكلمات الدالة:

روابط القص، الحمل-الانزلاق، موصلات مثقبة، مسامير القص، الربط الذاتي.